# ABSORPTION AND EMISSION CHARACTERISTICS OF DIFFUSE SPHERICAL ENCLOSURES

by

E. M. Sparrow

V. K. Jonsson

Heat Transfer Laboratory

Department of Mechanical Engineering

University of Minnesota

Minneapolis 14, Minnesota

This research was sponsored by the National Aeronautics and Space Administration (Grant NsG 137-61) under the technical supervision of Mr. S. Lieblein, Chief, Flow Processes Branch of the NASA Lewis Research Center.

## INTRODUCTION

The thermal radiation characteristics of spherical cavities are of practical interest in connection with the absorption of radiant energy for both space-vehicle and terrestrial applications. Also, spherical cavities are of potential use as sources of black-body energy. The purpose of this brief paper is to determine both the absorption and emission characteristics of spherical cavities which are diffuse reflectors and emitters.

An important aspect of the process of radiant interchange between surface elements in a diffuse spherical enclosure is that the angle factor[1] is independent of the orientation of the elements. In a spherical enclosure of radius R, the angle factor for radiation leaving any surface element 1 (area $A_1$) and incident on any other surface element 2 (area $A_2$) is

$$F_{1-2} = A_2 / 4\pi R^2 \tag{1}$$

and this holds whether $A_1$ and $A_2$ are infinitesimal or finite. Since the positions and orientations of the elements are not involved, it follows from equation (1) that energy leaving a typical element 1 is uniformly distributed over each unit area of the spherical enclosure. Additionally, it is seen that the energy incident on element 2 (from element 1) depends only on the ratio of its area $A_2$ to that of a complete sphere, $4\pi R^2$.

## ABSORPTION CHARACTERISTICS

General theory.--Consider a spherical enclosure of radius R having an opening defined by the angle $\varphi^*$ as pictured on figure 1. The surface area of the enclosure is denoted by $A^*$, and it is easily shown that

$$A^* = 2\pi R^2 (1 + \cos \varphi^*) \tag{2}$$

Radiant energy enters the cavity at a rate S (e.g., Btu/hr) and impinges on the surface with some arbitrary distribution given by $s(\varphi, \theta)$ per unit area.

---

[1] The angle factor is the fraction of the radiant energy leaving one surface element which is incident on some other surface element.

The angles $\varphi$ and $\theta$ are the polar and plane angles (respectively measured from the z and x axes) in a standard set of spherical coordinates.

Keeping account of the incoming energy, we note that an amount

$$\alpha S \tag{3a}$$

is absorbed at the first contact with the surface, and $(1-\alpha)S$ is reflected in all directions. Of this reflected energy, it follows from equation (1) that $(1-\alpha)S\,\frac{A^*}{4\pi R^2}$ remains within the enclosure and is uniformly distributed over the surface. Of the reflected energy which is thus incident on the surface, a fraction $\alpha$ is absorbed, i.e.,

$$\alpha S\left[(1-\alpha)\,\frac{A^*}{4\pi R^2}\right] \tag{3b}$$

and another fraction $(1-\alpha)\,\frac{A^*}{4\pi R^2}$ is re-reflected and then returns to the surface. Once again, a fraction $\alpha$ is absorbed, i.e.,

$$\alpha S\left[(1-\alpha)\,\frac{A^*}{4\pi R^2}\right]^2 \tag{3c}$$

and another fraction $(1-\alpha)\,\frac{A^*}{4\pi R^2}$ reflects and returns to the surface. If one were to keep account of all the successive absorptions, then the total energy absorbed could be obtained by simply summing the separate contributions as given by equations (3a), (3b), (3c), etc., thus

$$\alpha S\left\{1 + (1-\alpha)\,\frac{A^*}{4\pi R^2} + \left[(1-\alpha)\,\frac{A^*}{4\pi R^2}\right]^2 + \cdots\right\} \tag{4}$$

This is a geometric series whose sum is

$$\frac{\alpha S}{1 - 0.5\,(1-\alpha)(1+\cos\varphi^*)} \tag{5}$$

where $A^*$ has been replaced according to equation (2).

As a convenient representation of the absorption characteristics of the cavity as a whole, we introduce the apparent absorptivity which is defined as

$$\alpha_a = \text{(total absorbed energy)/(total incoming energy)} \tag{6}$$

Utilizing equation (5), it follows that

$$\alpha_a = \frac{\alpha}{1 - 0.5\,(1-\alpha)(1+\cos\varphi^*)} \tag{7}$$

The remarkable conclusion which follows from equation (7) is that the apparent absorptivity is independent of the detailed manner in which the incoming energy enters the enclosure. Therefore, equation (7) applies in general. The only parameters are the opening angle $\varphi^*$ and the surface absorptivity $\alpha$ .

The apparent absorptivity, as given by equation (7), has been plotted on figure 1 as a function of $\varphi^*$ for parametric values of $\alpha$ . Inspection of the figure reveals that the apparent absorptivity of the cavity always exceeds the surface absorptivity $\alpha$. The increase of $\alpha_a$ relative to $\alpha$ is greatest for surfaces of low absorptivity and for cavities with small openings (i.e., small $\varphi^*$). For very small values of $\varphi^*$, the apparent absorptivity is very close to unity regardless of the actual absorptivity of the surface.

Thus far, consideration has been given to the absorption characteristics of the enclosure as a whole. Now, attention will be directed to the energy absorbed locally at various positions on the enclosure surface. Let $\Lambda$ be the energy locally absorbed per unit area (e.g., Btu/hr-ft$^2$). To determine $\Lambda$ , we note that the incoming energy is distributed over the surface as given by $s(\varphi, \theta)$ per unit area (e.g., Btu/hr-ft$^2$). From the first contact of the incoming energy with the surface, the energy absorbed locally is

$$\alpha S \tag{8a}$$

However, all subsequent absorptions of reflected and re-reflected radiation take place uniformly at all locations in the enclosure. Therefore, from all absorptions following the first contact, the energy locally absorbed per unit area is simply obtained by subtracting $\alpha S$ from equation (5) and dividing by the surface area $A^*$, giving

$$\frac{\alpha(1-\alpha)\left(S/4\pi R^2\right)}{1 - 0.5\,(1-\alpha)(1+\cos\varphi^*)} \tag{8b}$$

Then, $\Lambda$ is obtained by adding equations (8a) and (8b),

$$\Lambda = \alpha S + \frac{\alpha(1-\alpha)\left(S/4\pi R^2\right)}{1 - 0.5\,(1-\alpha)(1+\cos\varphi^*)} \tag{9}$$

Clearly, the local distribution of the absorbed energy depends upon the detailed manner in which the incoming energy enters the enclosure, that is, on $s(\phi, \theta)$. For illustrative purposes, consideration will now be given to two interesting limiting situations.

Parallel rays.--Consider radiation arriving in a parallel ray bundle as illustrated in figure 2. The rays travel in the direction of the positive x-axis and make an angle $\beta$ with the vertical. The energy carried by the ray bundle may be characterized by $e_r$ per unit area normal to the ray[2] (e.g., Btu/hr-ft$^2$). Noting that the area of a surface tightly stretched across the opening of the spherical cavity is $\pi(R \sin \phi^*)^2$, and that the projection of the rays on the normal to this surface is accomplished by $\cos \beta$, it follows that the total energy S entering the enclosure is

$$S = e_r \pi R^2 \cos\beta \sin^2\phi^* \tag{10}$$

Next, it is necessary to find the surface distribution of the incoming energy as given by $s(\phi, \theta)$. Depending on the inclination angle $\beta$ and the opening angle $\phi^*$, the incoming rays may be directly incident only on part of the surface, the remaining portion receiving radiant energy due to internal reflections alone. Let us call the portion which is directly irradiated the no-shadow region, while the portion receiving only reflected energy will be called the shadow region. In the no-shadow region, the distribution function s (which is per unit surface area) may be derived by projecting the incoming rays along the surface normal. By writing expressions for unit vectors lying along the local surface normal (i.e., the radius vector) and the incoming rays, and then taking the scalar product, it is found that

$$s = e_r(\cos\theta \sin\phi \sin\beta - \cos\phi \cos\beta) \tag{11a}$$

in the no-shadow region. In the shadow region,

$$s = 0 \tag{11b}$$

---

[2]For example, the solar constant.

These expressions for s, along with equation (10) for $S_p$ may be utilized in determining the local distribution of the absorbed energy as given by equation (9).

In order to render equations (11) fully useful, it remains to determine the boundary between the shadow and no-shadow regions. To illustrate the method of analysis, consider the case where $\phi^* > 90°$, that is, a spherical shell smaller than a hemisphere. First of all, when the inclination angle $\beta < (\phi^* - 90°)$, the incoming radiation will fall directly on all parts of the surface (albeit non-uniformly). When $\beta > (\phi^* - 90°)$, a shadow region exists along with a region of direct illumination. The coordinates of the boundary curve between the shadow and no-shadow regions will be found with the aid of figure 2. The upper part of the figure is a plan view of the spherical shell showing radiation arriving from the right. The lower part of the figure is an elevation view cut through the spherical shell at a typical location y. A limiting ray which grazes the rim of the shell strikes the surface at a location x,z, and this is the boundary point between the shadow and no-shadow region. From the geometry of the figure

$$x = -r \cos(2\beta - \xi), \qquad z = -r \sin(2\beta - \xi) \tag{12a}$$

Also, it is easy to show that

$$r \sin\xi = -R \cos\phi^*, \qquad r \cos\xi = \sqrt{R^2 \sin^2\phi^* - y^2} \tag{12b}$$

Combination of equations (12a) and (12b) yields

$$x = R \cos\phi^* \sin 2\beta - \sqrt{R^2 \sin^2\phi^* - y^2} \cos 2\beta \tag{13}$$

$$z = -\sqrt{R^2 \sin^2\phi^* - y^2} \sin 2\beta - R \cos\phi^* \cos 2\beta$$

Equations (13) constitute a parametric representation of the boundary curve between the shadow and no-shadow regions.

When $\phi^* < 90°$ (spherical shell larger than a hemisphere), the boundary curve is also defined by limiting rays which graze the rim of the cavity opening and intersect the shell. But now, rays which graze at all points around the rim must be considered. From the rays which graze at the forward edge of the rim (toward the incoming rays), the x,z coordinates of the shadow, no-shadow boundary

remain as given by equations (13). From the rays which graze at the rearward edge of the rim, the boundary curve is found to be

$$x = R\cos\varphi^* \sin 2\beta + \sqrt{R^2\sin^2\varphi^* - y^2}\,\cos 2\beta$$
$$z = \sqrt{R^2\sin^2\varphi^* - y^2}\,\sin 2\beta - R\cos\varphi^*\cos 2\beta \qquad (14)$$

To provide some feeling for the nature of the boundary curve, it is useful to project it into the x-z and x-y planes. The projections have the following equations

$$x\sin 2\beta - z\cos 2\beta = R\cos\varphi^*$$
$$\frac{(x - R\cos\varphi^*\sin 2\beta)^2}{R^2\sin^2\varphi^*\cos^2 2\beta} + \frac{y^2}{R^2\sin^2\varphi^*} = 1 \qquad (15)$$

These projections are, respectively, a straight line and an ellipse. This indicates that the boundary curve cuts out a circle or a part of a circle on the surface of the spherical shell.

To illustrate these results, figure 3 has been prepared to show the projections of the boundary curve in plan and elevation views (x-y and x-z planes, respectively). The left-hand portion of the figure corresponds to an enclosure where $\varphi^*$ is greater than 90°. Projections are shown for inclination angles $\beta < 45°$, equal to 45°, and $> 45°$. The right-hand portion corresponds to $\varphi^*$ less than 90° and projections are shown for $\beta < 45°$ and equal to 45°. The case $\beta > 45°$ was not included in order to preserve clarity of the figure.

Diffuse incoming radiation.—Consider diffuse radiant energy uniformly distributed over the opening of the spherical cavity. The energy carried by the diffuse stream may be characterized by $e_d$ per unit area of the cavity opening. Without loss of generality, this energy may be regarded as coming from a black, isothermal spherical cap of radius R and emissive power $e_d$ which fits over the opening of the cavity. From this and from the corollaries of equation (1), it follows that the diffuse energy which enters the cavity is uniformly distributed along the surface of the cavity. Then, noting that the area of the cavity opening is $\pi(R\sin\varphi^*)^2$, we can write

$$S = e_d \pi R^2 \sin^2\varphi^* \qquad (16a)$$

$$S = S/A^* = 0.5\, e_d \sin^2\varphi^* / (1 + \cos\varphi^*) \qquad (16b)$$

Introducing this information into equation (9) gives the following result for the local absorbed energy

$$\Lambda = e_d \frac{0.5\alpha \sin^2\varphi^* / (1+\cos\varphi^*)}{1 - 0.5(1-\alpha)(1+\cos\varphi^*)} \qquad (17)$$

## EMISSION CHARACTERISTICS

Consideration is now given to the emission characteristics of a diffuse, isothermal spherical enclosure at temperature T. External radiation entering the enclosure is not included in the following analysis, but may be accounted for without difficulty.

The energy leaving any point on the surface per unit time and area (the radiosity B) is equal to the sum of the emitted energy plus the reflected portion of the incident energy. As shown in reference 1, the energy incident at any given point is obtained by taking the energy leaving another point, multiplying by an appropriate angle factor, and then integrating over the entire surface. So,

$$B(\varphi_0, \theta_0) = \epsilon\sigma T^4 + (1-\alpha)\int_{A^*} B(\varphi, \theta)\, dF \qquad (18)$$

in which the reflectivity has been replaced by $1 - \alpha$. Due to the symmetry of the problem, B will be uniform over the surface. Then, the solution of equation (18) immediately follows as

$$B/\sigma T^4 = \frac{\epsilon}{1 - 0.5(1-\alpha)(1+\cos\varphi^*)} \qquad (19)$$

where the angle factor has been taken from equation (1) with $A_2 = A^*$.

If the enclosure is to be used as a black-body cavity, then $B/\sigma T^4$ is a measure of its effectiveness. Clearly, it would be desired that $B/\sigma T^4$ approach as closely as possible to unity. If $\epsilon \approx \alpha$ (gray body), then $B/\sigma T^4$ can be read directly from figure 1. The figure reveals that a spherical enclosure with a small hole (small $\varphi^*$) is a very effective black body. If $\alpha \neq \epsilon$, then figure 1 may still be used, but the values read from the ordinate must be multiplied by $\epsilon/\alpha$.

The net local heat transfer rate q per unit surface area, which is the difference between the emitted energy $\epsilon\sigma T^4$ and the absorbed incident energy, is readily calculated to be

$$q = \epsilon\sigma T^4 \quad \frac{0.5 \sin^2\varphi^*/(1+\cos\varphi^*)}{1-0.5(1-\alpha)(1+\cos\varphi^*)} \tag{20}$$

The rate Q at which energy streams outward from the enclosure is obtained by multiplying equation (20) by the surface area $A^*$. A convenient representation of the overall heat transfer results may be made in terms of an apparent emissivity $\epsilon_a$. This is defined as the ratio of the actual rate at which energy streams from the enclosure to the energy emitted by a black circular disk having the same area as the opening of the cavity. The emission of such a disk is $\sigma T^4 \pi R^2 \sin^2\varphi^*$. Then, multiplying equation (20) by $A^*$ and dividing by the foregoing emission quantity gives

$$\epsilon_a = \frac{\epsilon}{1-0.5(1-\alpha)(1+\cos\varphi^*)} \tag{21}$$

For $\alpha \doteq \epsilon$, comparison of this expression with equation (7) shows that the apparent emissivity and apparent absorptivity of a spherical cavity are identical. Therefore, values of $\epsilon_a$ may be read directly from figure 1. If $\alpha \neq \epsilon$, the ordinates are to be multiplied by $\epsilon/\alpha$.

REFERENCE

1. E. M. Sparrow, J. L. Gregg, J. V. Szel, and P. Manos, "Analysis, Results, and Interpretation for Radiation Between Some Simply-Arranged Gray Surfaces," Trans. ASME, Journal of Heat Transfer, vol. 83, 1961, pp. 207-214.

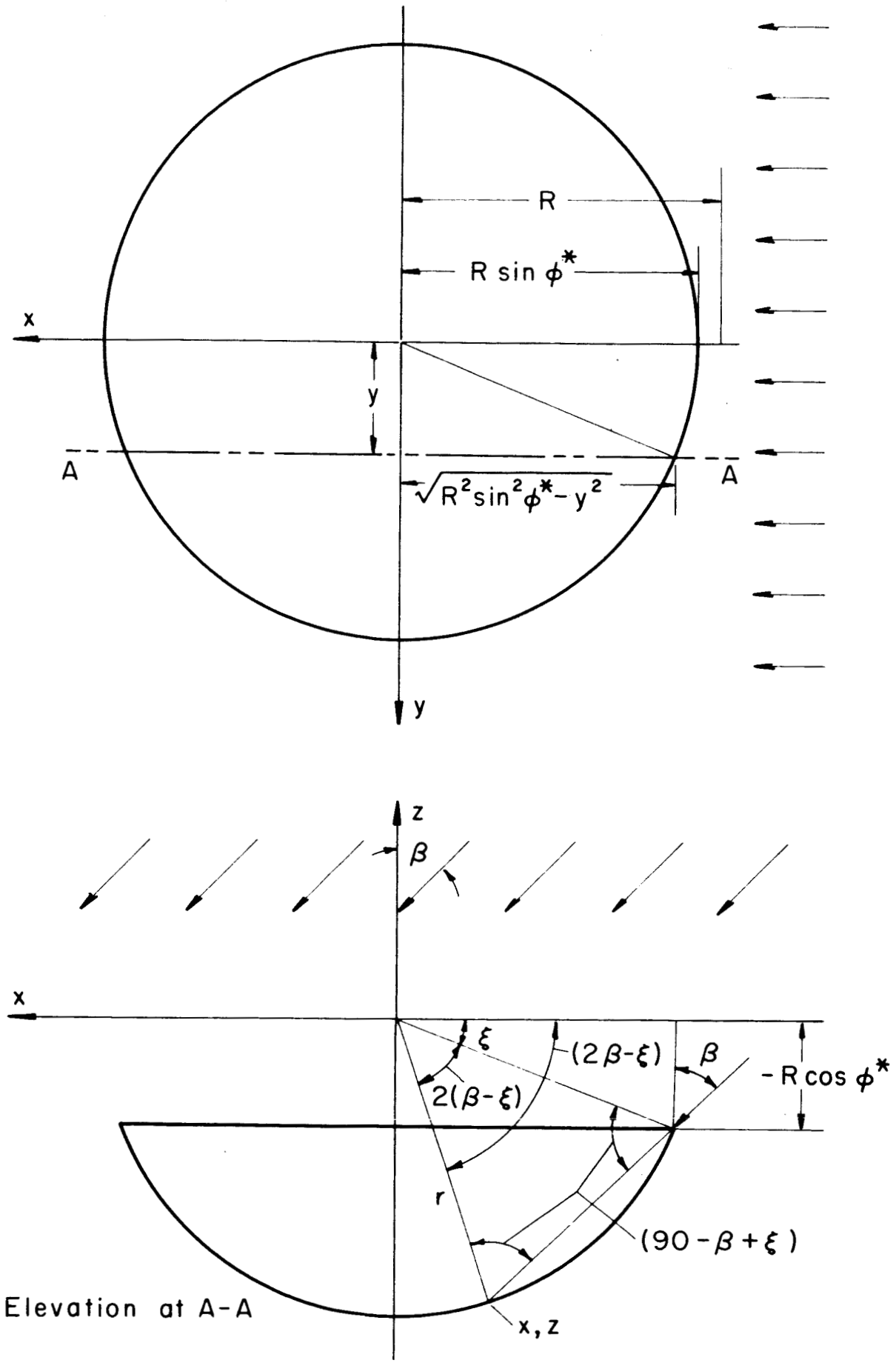


Fig. 2 Diagram for determining boundary between shadow and non-shadow regions, $\phi^* > 90°$

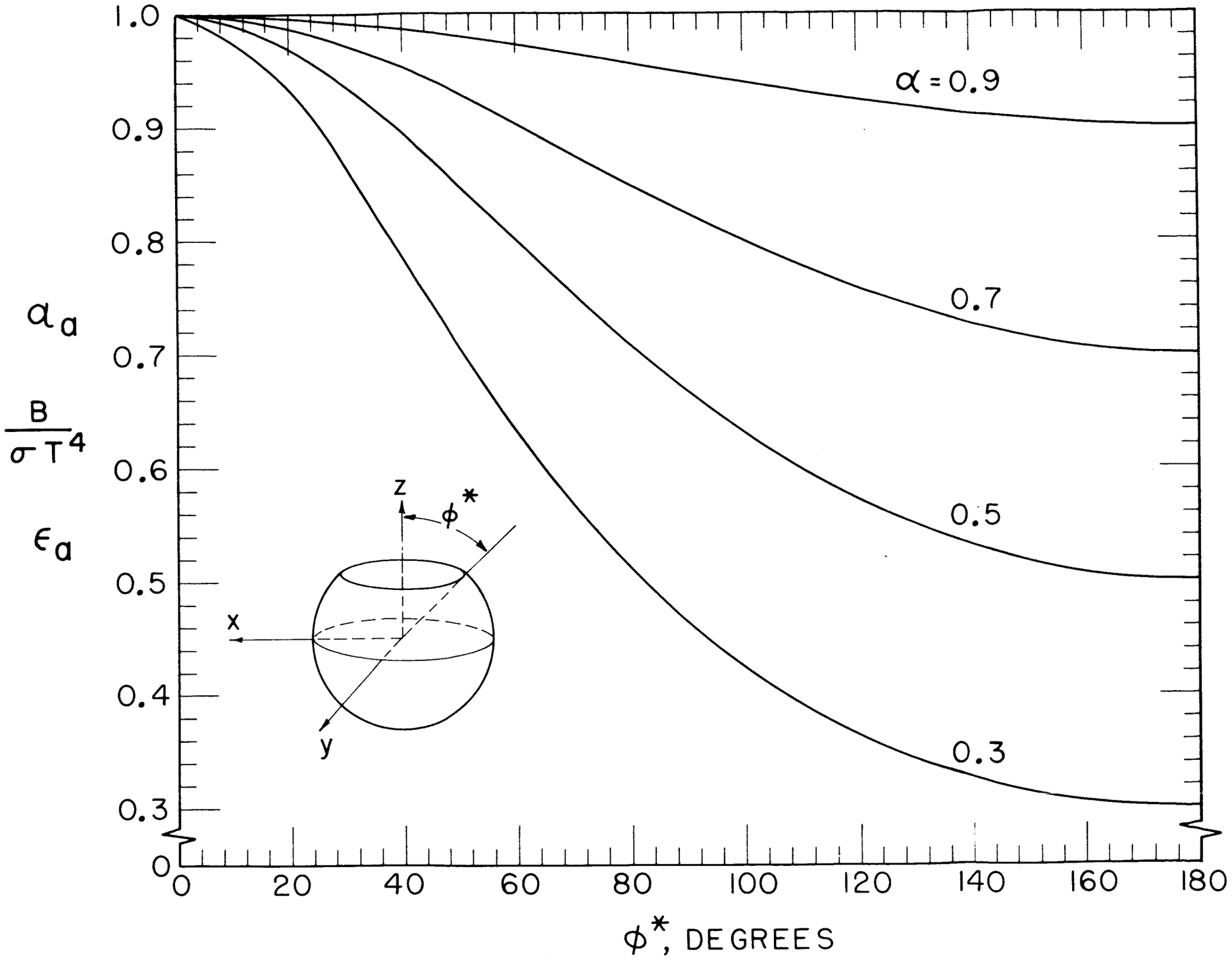


Fig. 1 Absorption and Emission Characteristics

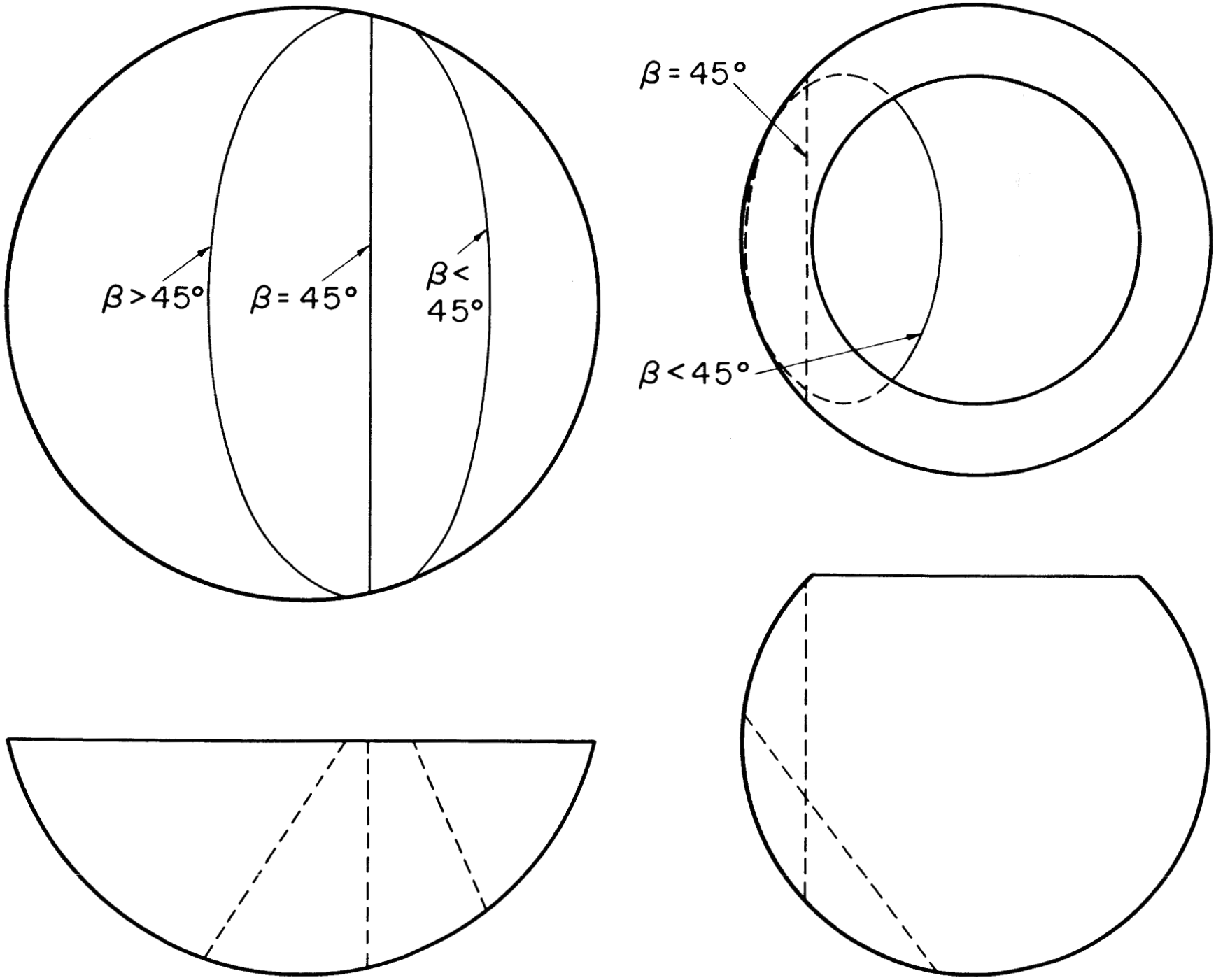


(a) LESS THAN HEMISPHERE

(b) LARGER THAN HEMISPHERE

Fig. 3 Projections of shadow, no-shadow boundary on plan and elevation views